Science Advances
AAAS

advances.sciencemag.org/cgi/content/full/5/6/eaaw0304/DC1

Supplementary Materials for

The cold Leidenfrost regime

Philippe Bourrianne*, Cunjing Lv, David Quéré*

*Corresponding author. Email: philippe.bourrianne@gmail.com (P.B.); david.quere@espci.fr (D.Q.)

Published 28 June 2019, *Sci. Adv.* **5**, eaaw0304 (2019)
DOI: 10.1126/sciadv.aaw0304

This PDF file includes:

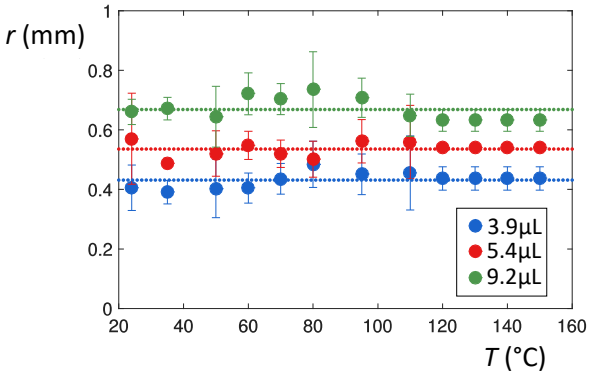

Fig. S1. Contact radius *r* of a water drop placed on a hot superhydrophobic solid, as defined in Fig. 2A. The substrate is Glaco-treated brass brought at temperature *T*. Three drop volumes are investigated: $\Omega = 3.9$ µL (blue), $\Omega = 5.4$ µL (red) and $\Omega = 9.2$ µL (green). The contact radius is found to be roughly independent of the substrate temperature.

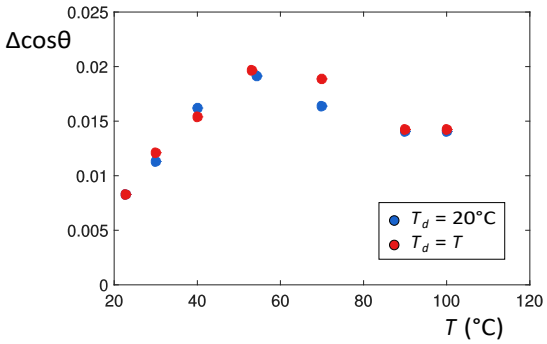

Fig. S2. Contact angle hysteresis Δcosθ on Glaco-coated substrates as a function of *T* for drops having initially either a temperature $T_d = 20$°C (blue data) or the same temperature as the substrate ($T_d = T$, red data). Regimes of adhesion appear to be independent of the drop initial temperature.

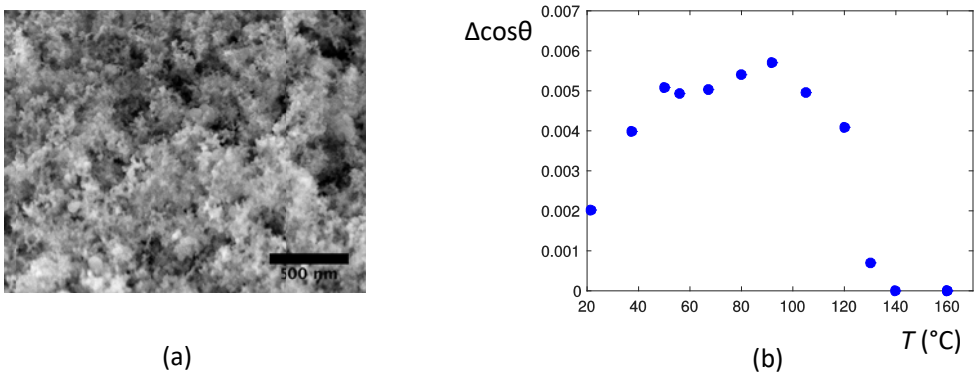

Fig. S3. Water adhesion on heated brass coated by a commercial colloidal repellent material (Ultra-Ever Dry, UltraTech International). (**A**) SEM picture of the surface of the samples (credits: Anaïs Gauthier). (**B**) Contact angle hysteresis Δcosθ for a millimetre-sized water drop as a function of the substrate temperature *T*. We observe the same sequence of regimes as in figure 2c.

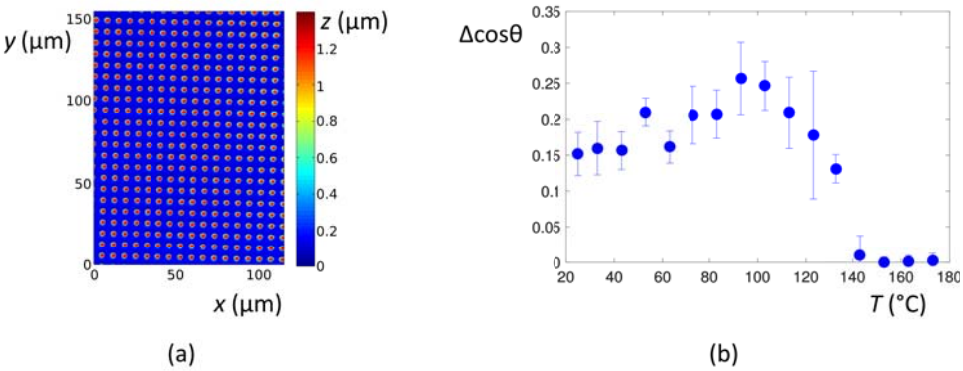

Fig. S4. Water adhesion on heated micrometric posts. (**A**) Profilometry of the substrate: a silicon wafer etched by Deep Reactive Ion Etching (DRIE) has micro-posts with diameter 2.6 μm, spacing 6.25 μm and height 1.2μm. (**B**) Contact angle hysteresis Δcosθ as a function of temperature *T*. We observe the same regimes as in figures 2c, SI-2 and SI-3, even if adhesion is much larger here, owing to a stronger pinning on micropillars.

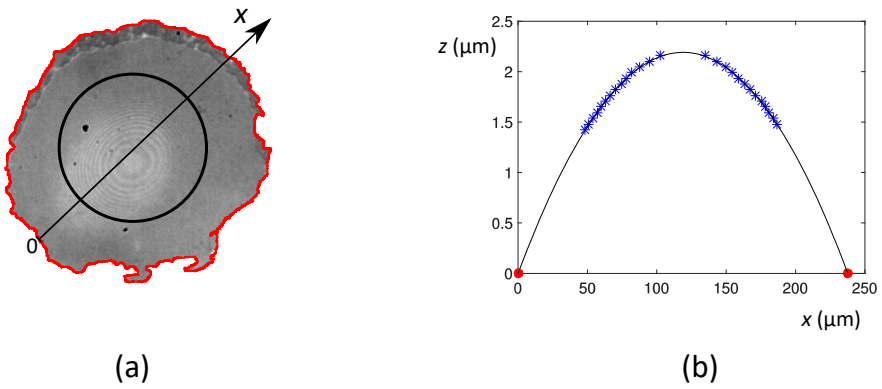

Fig. S5. Morphology of a vapor patch. (**A**) Fringes at the centre of the main vapor patch observed in figures 4b and 4c at $T = 75°C$. (**B**) We deduce from these fringes the location of the liquid/vapor interface (blue data), which appears to be nicely fitted by a circle (solid line) far from the contact line, in spite of pinning at the contact line. The intersection of this profile with the (red) contact line observed in (a) provides a vapor contact angle $\theta_v = 2°$. This very low value implies a weak contact angle hysteresis $\Delta\cos\theta_v$, yet large enough to generate visible distortion of the contact line. A low θ_v is typical of a superhydrophobic material, and it explains that even a small quantity of vapor (here about 30 pL) can invade macroscopic distances (here about a quarter of a millimeter) at the solid/water interface.

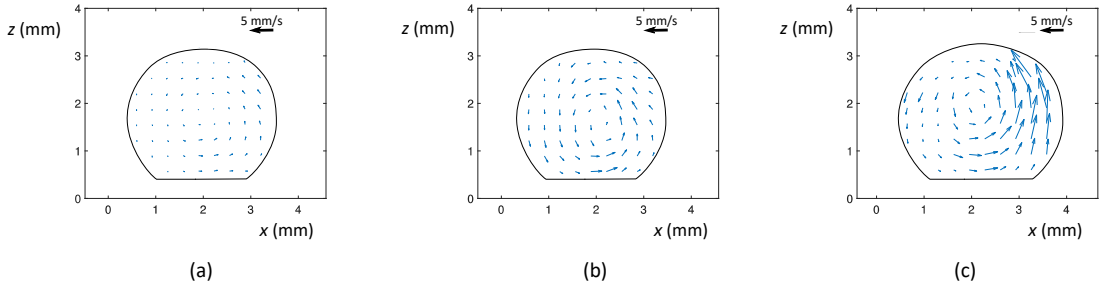

Fig. S6. Internal flow in water drops ($R \approx 1.5$ mm) placed on a hot superhydrophobic solid (Glaco-coated wafer). Observations are performed by PIV (particle image velocimetry) at different solid temperature. In all cases, an inner motion is observed and found to consist in a rolling motion, a symmetry breaking we attribute to confinement. The scale of the velocity vectors is the same in all pictures and given by the bold arrow showing 5 mm/s. (**A**) At $T = 50°C$, the average and maximum measured velocities of water inside the drop are around 0.5 mm/s and 1 mm/s, respectively. (**B**) At $T = 85°C$, the average and maximum velocities are around 1.1 mm/s and 2.5 mm/s. (**C**) At $T = 107°C$, the average and maximum velocities are around 2.4 mm/s and 7.1 mm/s.